

field. With mean-field indices  $\beta = \frac{1}{2}$ ,  $\Delta = \frac{3}{2}$ , Eq. (14) becomes the usual mean-field equation of state, and  $M_\phi$  vanishes linearly with  $h$ .

In the case when the specific heat has a logarithmic singularity, Eq. (12) is replaced by

$$\frac{\epsilon^*}{\epsilon} = 1 + A \frac{h}{\epsilon^\Delta} \left( \frac{\epsilon^*}{\epsilon} \right)^{1-\Delta} \frac{1}{\ln[(\epsilon^*)^{-1}]}. \quad (15)$$

Since  $\epsilon^*/\epsilon$  is not a function of  $h/\epsilon^\Delta$  alone,  $M_\phi$  is not of the homogeneous form assumed in scaling theories. However, the linear scaling relations among the indices are still satisfied. When  $h/\epsilon^\Delta \ll 1$ ,  $\epsilon^* \approx \epsilon$ , so  $h/\epsilon^\Delta \ln(\epsilon^{-1})$  is a good approximate scaling variable. This shows<sup>14</sup> that for  $T < T_c$ ,  $\chi_\phi \approx D\epsilon^{\beta-\Delta}/\ln(\epsilon^{-1})$ , as  $\epsilon \rightarrow 0$ . For  $h/\epsilon^\Delta \gg 1$ ,  $\epsilon^* \approx (Ah)^{1/\Delta}$ , so  $h/\epsilon^\Delta \ln[(Ah)^{-1/\Delta}]$  is a good scaling variable in this region. Consequently, when  $\epsilon = 0$ ,  $M_\phi^{\Delta/\beta} \approx \tilde{D}h/\ln[(Ah)^{-1/\Delta}]$  as  $h \rightarrow 0$ . For the square Ising lattice,  $\beta = \frac{1}{8}$ ,  $\Delta = \frac{15}{8}$ , and the coefficients  $D = 0.0208$  and  $\tilde{D} = 2.77$  can be evaluated from Onsager's<sup>5</sup> free energy and Yang's spontaneous magnetization. The logarithms appearing in these asymptotic forms for  $\chi_\phi$  and  $M_\phi$  are a result of our approximation, and are not believed to be present in the actual solution of the two-dimensional Ising model.

We are grateful to Dr. G. Baker and Dr. G. Stell for their help in finding the relevant literature on the series-expansion results. We would

like to thank Dr. B. McCoy for many interesting discussions.

\*Work supported in part by the National Science Foundation under Grant No. GP-32998X.

†Work at Brookhaven National Laboratory performed under the auspices of the U. S. Atomic Energy Commission.

<sup>1</sup>M. E. Fisher, Rep. Progr. Phys. **30**, 615 (1967); L. P. Kadanoff, Physics (Long Is. City, N. Y.) **2**, 263 (1966); B. Widom, J. Chem. Phys. **43**, 3892 (1965).

<sup>2</sup>See, e.g., R. B. Griffiths, J. Math. Phys. (N. Y.) **5**, 1215 (1964); H. Falk, Amer. J. Phys. **38**, 858 (1970).

<sup>3</sup>See, e.g., M. Blume, V. J. Emery, and R. B. Griffiths, Phys. Rev. A **4**, 1071 (1971).

<sup>4</sup>To be precise, we add to  $H_0$  a small magnetic field  $h'' > 0$ . Then, after inserting  $H_0$  into Eq. (1), we first take the limit  $N \rightarrow \infty$ , and then let  $h'' \rightarrow 0+$ .

<sup>5</sup>L. Onsager, Phys. Rev. **65**, 117 (1944).

<sup>6</sup>C. N. Yang, Phys. Rev. **85**, 808 (1952).

<sup>7</sup>D. S. Gaunt and C. Domb, J. Phys. C: Proc. Phys. Soc., London **3**, 1442 (1970).

<sup>8</sup>M. F. Sykes, J. W. Essam, and D. S. Gaunt, J. Math. Phys. (N. Y.) **6**, 283 (1965).

<sup>9</sup>D. Mattis and M. Plischke, J. Math. Phys. (N. Y.) **10**, 1107 (1969).

<sup>10</sup>G. S. Rushbrooke, J. Chem. Phys. **39**, 842 (1963).

<sup>11</sup>R. B. Griffiths, J. Chem. Phys. **43**, 1958 (1965).

<sup>12</sup>J. T. Ho and J. D. Litster, Phys. Rev. Lett. **22**, 603 (1969).

<sup>13</sup> $C_H - T(\partial M/\partial T)^2 \chi^{-1} = C_M \geq 0$ ; see, e.g., Fisher, Ref. 1.

<sup>14</sup>This also follows from Eq. (7).

## Significant Deviation of Rotational Decay from Theory at a Reliability in the $10^{-12}$ sec<sup>-1</sup> Range\*

J. K. Fremerey

*Institute of Physical Chemistry, University of Bonn, 53 Bonn, Germany*

(Received 25 August 1972; revised manuscript received 2 February 1973)

New drag-versus-speed measurements with a freely spinning steel sphere in a cavity-type permanent-magnet suspension confirm the up-to-date theories of residual drag (Coriolis, eddy-current, and relaxation effects). A small excessive drag is of particular interest for the discussion of Keith's gravitational radiation effect.

The investigation of the residual drag torque on magnetically suspended rotors<sup>1-7</sup> was particularly promoted due to the predictions of Keith on the effect of gravitational radiation.<sup>8,9</sup> According to Keith, the associated energy loss would cause a rotor deceleration of the order  $10^{-11}$  sec<sup>-1</sup> in the case of a 2.5-mm-diam sphere at rim velocities of about 700 m/sec. In contrast to the generally accepted Einstein-Edding-

ton-Weber theory, Keith expects a damping effect also for axially symmetric rotors.

We have previously shown that, in accordance with another (nongravitational) theory of Keith's,<sup>3</sup> a residual drag of a few  $10^{-9}$  sec<sup>-1</sup> appears, due to Earth's rotation (Coriolis effect), if the rotor is suspended in a magnetic field of about 400 G.<sup>7</sup> The same theory, which also suggests how to account for geometry disturbances of the suspen-

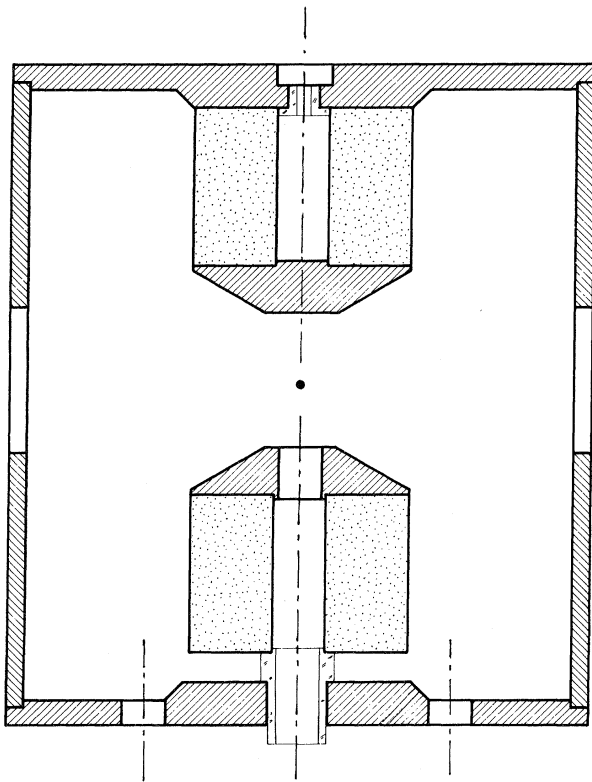


FIG. 1. Permanent magnet system (16 cm diam) for rotor suspension, with a 2.5-mm sphere at its equilibrium position.

sion field, shows that the Coriolis effect may be considerably reduced by a stronger coupling of the rotor spin to the magnetic field axis, i.e., by increasing the field at the rotor. These results, and the previously developed permanent-magnet suspension,<sup>10</sup> led to the construction of a cavity-type magnet system which provides a flux density  $B = 915 \pm 2$  G at the rotor equilibrium position (Fig. 1).

The rotational decay observations have been carried out with a 2.495-mm-diam ball-bearing sphere<sup>11</sup> at gas pressures below  $10^{-10}$  Torr, and at a temperature stability of about 1 mK.<sup>6</sup> The results are shown in Fig. 2. The measured decay ratio was appreciably larger than the Coriolis effect [see Fig. 2(a)]. The additional drag must be ascribed to eddy-current losses due to the rotating component  $\vec{m}_\perp$  of the rotor magnetization. This type of drag has been observed even with open-magnet designs, where special care had been taken to keep the distance between the rotor and conducting parts of the apparatus large,<sup>6</sup> and it will have more influence in the new type of suspension because of the smaller distances.

It is easy to show that the decay ratio is proportional to the power dissipation involved, and that the latter is proportional to the square of  $\vec{m}_\perp$ , which may be determined by measuring the "dynamo voltage"  $U$  induced at the drive coils<sup>6</sup> (this voltage controls the time-measuring system as well<sup>10</sup>). The rotating moment  $\vec{m}_\perp$  is relatively large when the rotor is accelerated for the first time after having been suspended, and is decreased by the effect of the rotor drive during the successive acceleration/deceleration cycles.<sup>6</sup> One may thus obtain several values of the decay ratio and of the corresponding dynamo voltage for the same frequency. In most cases, we have recorded three values of each [see Fig. 2(a)]. Because of the quadratic relation between the decay ratio and the dynamo voltage, the corresponding values of Fig. 2(a) can be reduced according to, e.g.,

$$-\frac{\dot{\omega}}{\omega} = \frac{(U_A/U_B)^2(-\dot{\omega}/\omega)_2 - (-\dot{\omega}/\omega)_1}{(U_A/U_B)^2 - 1} \quad (1)$$

in order to eliminate the effect of  $\vec{m}_\perp$ .

Most of the reduced values come down very closely above the theoretical curve, which represents the Coriolis effect at zero field asymmetry,

$$(-\dot{\omega}/\omega)_0 = \theta_0^2 / \tau [1 - k_\eta (a\omega/c_s)^2], \quad (2)$$

where  $\theta_0$  denotes the equilibrium hang-off angle between the rotor spin and the magnetic field axis, due to Earth's rotation, and  $\tau$  is the time constant of the equilibrium approach.<sup>3,7,11</sup> A small negative correction term accounts for the elastic rotor deformation due to centrifugal forces, where  $k_\eta \approx 0.6$  involves Poisson's ratio,  $a\omega$  is the equatorial speed, and  $c_s$  denotes the speed of sound within the rotor material.<sup>12</sup>

The deviations of the reduced experimental points from the theoretical curve (2) are plotted on an expanded ordinate scale in Fig. 2(b). The open circles result from combining branches 1, 2, A, B of Fig. 2(a) according to (1). The remarkable drop of these values toward high frequencies may be related to relaxation processes. In a previous paper<sup>6</sup> we have discussed the shifting of the rotor magnetization (this process starts at low frequencies, and may be recognized by a settling down of the dynamo voltage), and the plastic flow of the rotor material, which appears at high frequencies due to internal stresses.<sup>13</sup> Such processes are accompanied by energy losses which enhance the decay ratio. As the magnetic relaxations are promoted by the rotor drive,<sup>6</sup>

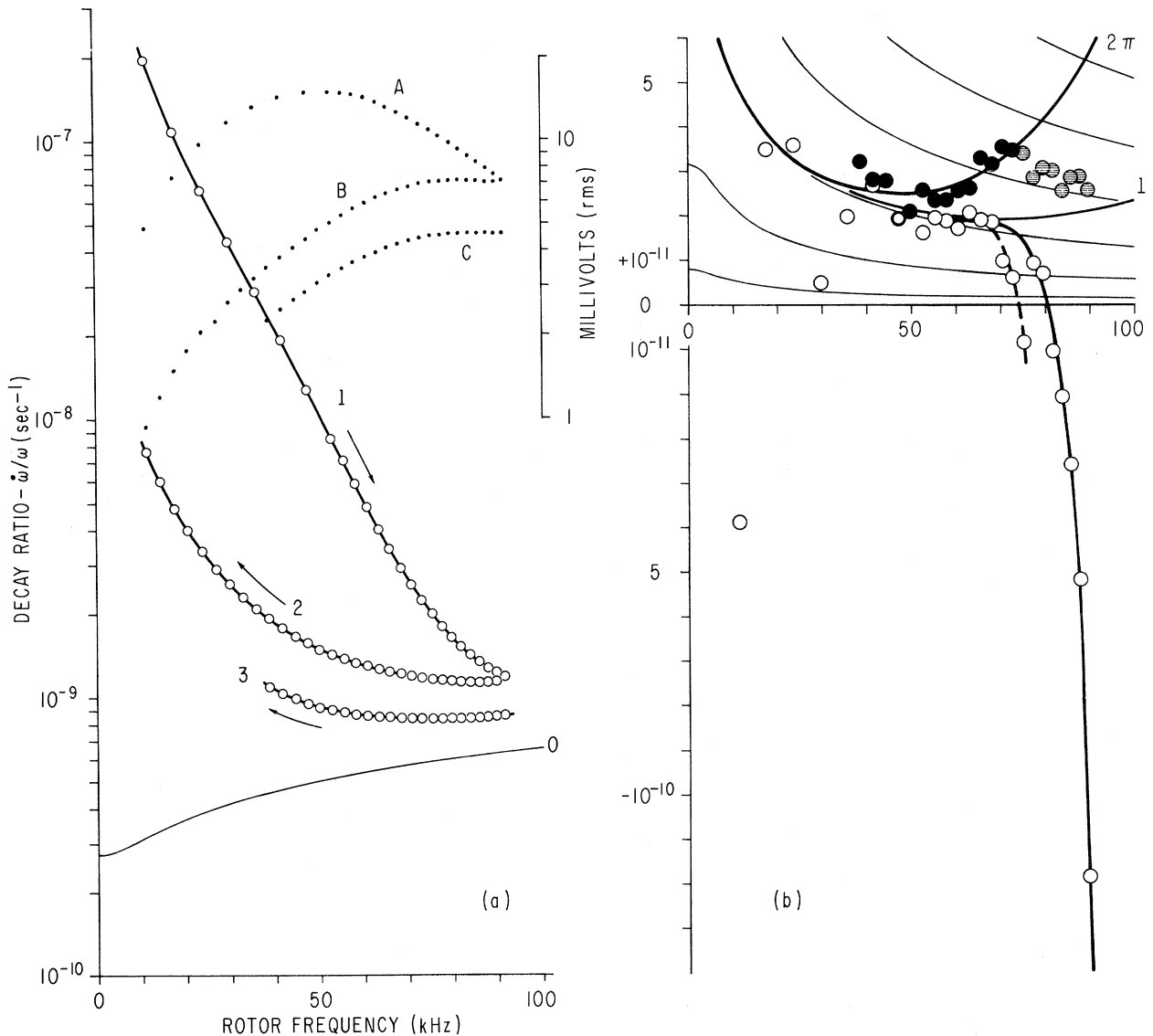


FIG. 2. Rotational decay observations from a 2.5-mm ball bearing sphere. (a) Three branches of the decay ratio (1, 2, 3), and the simultaneously recorded dynamo voltages (A, B, C). The bottom curve represents the theoretical Coriolis effect at zero field asymmetry. (b) Deviations of the reduced values (exterior eddy current losses eliminated) from the bottom curve in (a). The weak lines belong to constant field asymmetries (1 ppm spacing). The labeled curves represent the gravitational Keith effect (3.05-ppm field asymmetry), with either  $k'=1$  (Birkhoff) or  $k'=2\pi$  (Einstein).

they become successively smaller when turning over to another frequency. Therefore, the corresponding drag was larger at the first branch than at the second, and still lower at the third, and we always obtain an overcompensation of the exterior eddy-current losses (due to  $\vec{m}_\perp$ ) when using Eq. (1). Similar considerations apply in the case of the strain relaxations (predominant at  $\omega/2\pi > 70$  kHz), which are promoted by running the rotor still farther beyond the stretching

strain limit (branches No. 3, C have been recorded after a short run at 100 kHz). The presence of relaxation processes is even more emphasized by the fact that those points of the first branch in Fig. 2(a), which contribute to the three points on the broken curve in Fig. 2(b), were recorded half a day after switching off the rotor drive, whereas all the following points were recorded after a whole day of free rotation.

The multiple-branch recording of the decay

ratio is a highly sensitive method for detecting the described relaxation processes, and it is important to note that when a small effect which increases with  $\omega$  (such as the Keith effect) is to be looked for, this method may only obscure the effect rather than simulate it.

The filled circles in Fig. 2(b) denote those values which result from working with branches 2, 3, B, C of Fig. 2(a). Since this time the rather strong relaxations of the first branch are not involved, we expect a much weaker drop of the reduced values with regard to the "equilibrium" decay ratio, which is not affected by relaxations. Indeed, at frequencies between 50 and 70 kHz, the decay ratio now increases with  $\omega$  instead of being nearly constant, and the strain-related drop above 70 kHz (shaded circles) does not produce negative deviations from the Coriolis effect (2).

From the up-to-date theories of residual drag,<sup>3,7</sup> we would expect a downward trend of the filled circles in correspondence with the field asymmetry level lines. The significant upward trend of these points seems to indicate the existence of a small real excessive drag which strongly increases with the rotor speed. We shall now discuss some phenomena which obviously may be thought of when additional rotor drag is to be considered.

It had previously<sup>3</sup> been suggested that shape deviations and unequal moments of inertia of the sphere might cause additional eddy-current drag. Of course, the appearance of the rotating component  $\vec{m}_\perp$  of the rotor magnetization, and the mutual shift of the rotor spin and magnetization have to be regarded as being due to the above phenomena.<sup>6</sup> We have already considered the additional drag due to the exterior eddy currents induced by  $\vec{m}_\perp$ . It is easy to show that, because of the rapid change (at high rotor speeds) of the direction of the magnetic torque associated with  $\vec{m}_\perp$ , the resulting (slowly relaxing) spin-axis deviations are so small that the effect of interior eddy currents (induced at the sphere itself)<sup>3,7</sup> may be neglected.

The electromagnetic radiation damping due to  $\vec{m}_\perp$  corresponds to a decay ratio of less than  $10^{-23} \text{ sec}^{-1}$ .

It can be shown from elementary theory that the radiation damping due to electric surface charges on the sphere is negligible unless the rotor potential exceeds the million-volt range, and drags due to a rotating-charge-induced magnetic moment are negligible even compared to

radiation damping.

The electric and magnetic properties of the rotor material<sup>11</sup> within the surface region of the sphere (the interior regions are shielded against high-frequency alternating fields due to the skin effect) may be regarded as constant, i.e., they do not change enough due to the elastic deformations of the rotor material to have a significant effect on our experiments. This statement has been proved experimentally with cylindrical steel probes under axial stress.

The residual gas friction at pressures below  $10^{-10}$  Torr has a smaller effect than the considered one, and the associated decay ratio is independent of  $\omega$ .<sup>1,10</sup>

The effect of the residual lateral rotor vibrations decreases with increasing rotor speed, as may be concluded from a previous discussion,<sup>7</sup> its magnitude being comparable with the scatter of the experimental points. The scatter is much smaller than the effect considered, and, in the higher frequency region, amounts to only a few  $10^{-12} \text{ sec}^{-1}$ . This is, at present, the overall reliability of the new instrument and method.

Errors in the determination of the experimental parameters entering the Coriolis effect (2) may cause a vertical shift of all values in Fig. 2(b) by less than  $5 \times 10^{-12} \text{ sec}^{-1}$  without affecting the characteristics of their frequency dependence.

We cannot give a conclusive explanation of the detected effect after the preliminary observations described in this paper. However, the reliability of the experimental results seems to allow the conclusion that we have observed a real additional drag on top of that which can be explained by well-known theories, and it seems interesting that the filled circles in Fig. 2(b) are quite a good fit to the upper bold curve which represents the gravitational Keith effect, with  $k' = 2\pi$ ,<sup>14</sup> at a field asymmetry of about 3 ppm.

The author is much indebted to Professor Dr. Wilhelm Groth for his support.

\*Work supported by the Deutsche Forschungsgemeinschaft.

<sup>1</sup>J. W. Beams, D. M. Spitzer, Jr., and J. P. Wade, Jr., *Rev. Sci. Instrum.* **33**, 151 (1962).

<sup>2</sup>D. M. Spitzer, dissertation, University of Virginia, 1962 (University Microfilms, Ann Arbor, Mich., 1962).

<sup>3</sup>J. C. Keith, *J. Res. Nat. Bur. Stand., Sect. D* **67**, 533 (1963).

<sup>4</sup>J. D. Nixon and D. J. Kenney, *Rev. Sci. Instrum.* **35**, 1365 (1964).

<sup>5</sup>J. D. Nixon and D. J. Kenney, *Rev. Sci. Instrum.* **35**,

1721 (1964).

<sup>6</sup>J. K. Fremerey, *Rev. Sci. Instrum.* **42**, 753 (1971).

<sup>7</sup>J. K. Fremerey, *Rev. Sci. Instrum.* **43**, 1413 (1972).

The discrepancies between the experimental points and the theoretical curves in this paper result from erroneous values which have been inserted for some of the experimental parameters.

<sup>8</sup>J. C. Keith, *J. Math. Phys. (N. Y.)* **42**, 248 (1963).

<sup>9</sup>J. C. Keith, *Rev. Mex. Fis.* **12**, 1 (1963).

<sup>10</sup>J. K. Fremerey, *J. Vac. Sci. Technol.* **9**, 108 (1972).

<sup>11</sup>The reversible permeability  $\mu_r = 44.5$ , the resistivity  $1/\sigma = 28.0 \times 10^{-6} \Omega \text{ cm}$ , and the density of the rotor ma-

terial  $\rho = 7.79 \text{ g/cm}^3$ , which all are involved in  $\theta_0$  and  $\tau$  (see Ref. 7), have been determined with a cylindrical probe after a 6-h bake at  $400^\circ\text{C}$ . The sphere had been treated similarly during outgassing of the vacuum system.

<sup>12</sup>G. Comsa and J. K. Fremerey, to be published.

<sup>13</sup>The associated relaxation has been observed more directly by the author [dissertation, University of Bonn, 1969 (unpublished)].

<sup>14</sup>The  $k'$  parameters 1 and  $2\pi$  involve the feedback coefficient of the universe as calculated according to Birkhoff or Einstein, respectively (see Ref. 9).

## Further Measurements of the Submillimeter Background at Balloon Altitude\*

Dirk J. Muehlner and Rainer Weiss

*Research Laboratory of Electronics and Department of Physics, Massachusetts Institute of Technology, Cambridge, Massachusetts 02139*

(Received 9 March 1973)

Measurements of the far-infrared background radiation were made with a balloon-borne radiometer at an altitude of 44 km. Equivalent blackbody temperatures of  $2.55^{+0.25}_{-0.45}$ ,  $2.45^{+0.45}_{-1.05}$ , and  $2.75^{+0.8}_{-2.75}$  K were obtained for the background radiation in bandwidths extending from 1 to 11.5, 13.5, and 18.5  $\text{cm}^{-1}$ . The total measured flux in the largest bandwidth is dominated by the atmospheric emission by ozone and water. The radiation of these atmospheric components was determined independently in a separate pair of radiometer spectral responses.

This Letter reports the results of a balloon flight made on 1 October 1972 from the National Center for Atmospheric Research (NCAR) Scientific Balloon Facility at Palestine, Texas. The results of earlier flights and a description of the instrument have been published.<sup>1</sup> There were several differences between this and previous flights.

(1) The radiometer had new filters which gave the overall system responses shown in Fig. 1. SR1 is the same as in previous flights. SR2 and SR3 are determined by sharp-cutoff low-pass capacitive-grid interference filters with cutoff frequencies chosen to reject atmospheric radiation. SR4 and SR5 are determined by two-element capacitive-grid filters with transmission peaks at the  $22\text{-cm}^{-1}$  Q branch of ozone and the  $18.6\text{-cm}^{-1}$  water line. The purpose of these narrow-band filters was to allow specific measurements of the ozone and water radiation, which are used to subtract the atmospheric contributions to the signals in the other spectral responses. This procedure is intended to supplement zenith scanning, which can only give a lower limit for the atmospheric contribution.

(2) The measurements were carried out at 44

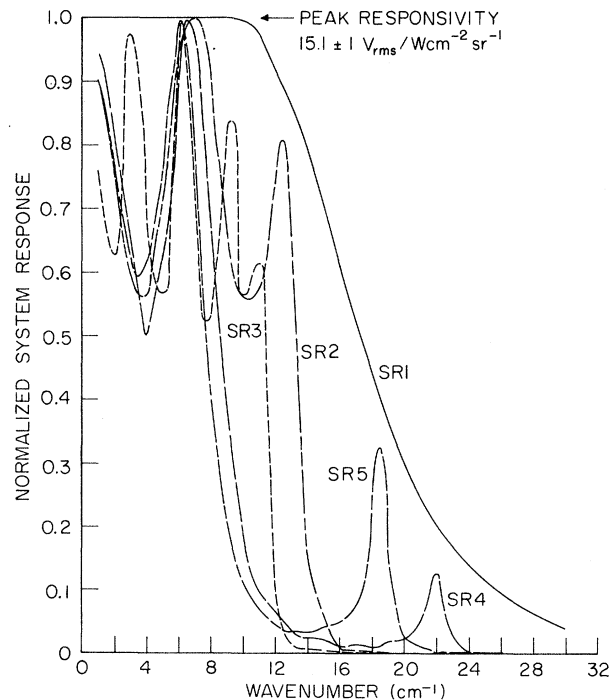


FIG. 1. Spectral responses of radiometer.